

HelioPure:

A Multi-Stage Photocatalytic-Ion Exchange-Adsorptive System for Decentralized Surface Water Treatment

Author and Researcher: Aadit P. Krishna
Central Academy of Technology and Arts, Monroe, NC, USA

Stockholm Junior Water Prize
North Carolina State Competition 2026

Abstract

Over 2.2 billion people globally lack safely managed drinking water while per- and polyfluoroalkyl substances (PFAS) contaminate the supplies of more than 180 million Americans, resisting all conventional treatment. This paper presents HelioPure, a floating, solar-powered multi-stage purification system integrating immobilized anatase TiO_2 photocatalysis, strong-base anion exchange resin, granular activated carbon (GAC) adsorption, and fine filtration, designed and constructed independently from commercially available components at approximately \$165 without laboratory facilities. We hypothesized that this integrated system would achieve significantly greater reductions in turbidity, total dissolved solids (TDS), and PFAS than a GAC-and-filtration-only control under natural winter sunlight in Waxhaw, NC. Across three independent field trials, the full system achieved mean turbidity reduction of $78.4\% \pm 2.1\%$ and TDS reduction of $50.1\% \pm 1.9\%$, outperforming the GAC-only control by 15–22% ($p < 0.05$, two-sample t-test; Cohen's $d = 5.5$ and 4.3 respectively). Integration of the anion exchange stage reduced PFAS from 59.12 ± 3.54 ppt to 9.04 ± 1.67 ppt, an $84.8\% \pm 2.0\%$ mean removal ($p < 0.001$; $d = 14.9$). pH remained stable within potable limits. Conservative cost modeling suggests treated water production at \$0.001–0.005 per liter under assumed operational parameters. These results demonstrate that integrated solar-driven photocatalysis and ion exchange separation can address both conventional contamination and emerging PFAS in real untreated surface water using accessible materials, without laboratory resources or grid infrastructure. The system targets off-grid deployment in resource-limited settings, motivated by water insecurity in Tirunelveli, Tamil Nadu, India.

1. Introduction

1.1 The Global Water Crisis and Chemical Contamination

Approximately 2.2 billion people rely on drinking water sources contaminated with pathogens or hazardous chemicals, contributing to an estimated 1.2 million deaths annually [1]. The World Economic Forum's 2023 Global Risks Report ranked water crises among the top five global societal threats, reflecting the gap between the science of water treatment and its real-world deployment [7]. Existing low-cost decentralized solutions address this gap only partially. Solar disinfection (SODIS) can inactivate pathogens in PET bottles after 6+ hours of sunlight but removes no dissolved chemical contaminants [13]. Biosand filters reduce turbidity and fecal coliforms but lack mechanisms for synthetic chemical removal [14]. Commercial point-of-use devices such as LifeStraw primarily address

biological contamination at costs of \$15–30 per unit; none of these systems address PFAS or dissolved organics under off-grid conditions [7]. Chemical pollution has become an equally serious and more insidious threat than biological contamination in many settings. Agricultural runoff saturates freshwater systems with nitrates, phosphates, and pesticides; industrial discharge releases heavy metals and synthetic organic compounds; and PFAS (per- and polyfluoroalkyl substances) now contaminate the drinking water of more than 180 million Americans, with particular concentrations in North Carolina communities downstream of industrial discharge and firefighting foam sites [3]. PFAS are associated with cancers, immune suppression, thyroid disruption, and developmental toxicity, and resist every conventional treatment process due to the carbon–fluorine bond’s exceptional stability at approximately 485 kJ/mol [6]. The EPA’s 2023 maximum contaminant level of 4.0 ppt for individual PFAS - the most stringent drinking water regulation in U.S. history - cannot be met by any currently deployed portable treatment technology.

No single accessible treatment mechanism addresses this full contaminant spectrum. Boiling and chlorination are effective against pathogens but leave synthetic chemicals untouched. Reverse osmosis provides broad removal but demands 50–150 psi operating pressure, frequent maintenance, and infrastructure unavailable in off-grid settings [7]. GAC adsorption is kinetically effective for long-chain PFAS but requires Empty Bed Contact Times (EBCTs) of 5–25 minutes for meaningful removal [15], and captures but does not destroy contaminants, eventually saturating. TiO_2 photocatalysis generates hydroxyl radicals capable of oxidizing organic pollutants and inactivating pathogens, but has been limited in field deployment by nanoparticle release risks, limited UV absorption (~5% of solar spectrum), and the inability to mineralize PFAS under passive solar conditions alone [5, 10]. Strong-base anion exchange resins demonstrate effective PFAS capture through electrostatic and hydrophobic mechanisms in municipal applications [8, 9], but prior to this study had not been integrated into floating, solar-powered decentralized platforms. The gap: no affordable, off-grid, multi-contaminant system capable of addressing both physical turbidity and chemical PFAS contamination - is what HelioPure was designed to fill.

1.2 A Personal Motivation: Tirunelveli, India

This research did not begin in a laboratory. It began in Tirunelveli, Tamil Nadu, India, where my family has roots spanning generations. During an early visit, I watched family members collect water from a local lake, carry it home, and boil it before use. Boiling kills pathogens. It removes nothing of the trace industrial compounds, agricultural chemicals, and emerging contaminants increasingly documented in South Asian surface water systems. What those family members lacked was access to a treatment technology designed for their context: off-grid, affordable, deployable without infrastructure, and effective against chemical contamination. Critically, HelioPure was designed and built *without* university laboratory access, professional equipment, or institutional resources: only commercially available materials and independently acquired knowledge. This context is central to the project's relevance: a system that requires laboratory infrastructure to build cannot be deployed in Tirunelveli.

1.3 Research Lineage

HelioPure is the third project in a four-year arc of independently conducted water research. In 2022, Hu-RiFy demonstrated solar-powered atmospheric water generation. In 2024, PuriFAS demonstrated multi-stage PFAS filtration combining reverse osmosis with strong-base anion exchange resin, achieving 74% greater removal than either mechanism alone [16], earning the Samsung Solve for Tomorrow award and publication in the NSRI Student Research Journal affiliated with MIT Critical Data. HelioPure synthesizes both: solar autonomy from Hu-RiFy, multi-stage integration from PuriFAS, adding TiO₂ photocatalysis as an active oxidative pretreatment stage on a floating, field-deployable platform. All three generations were conducted without laboratory facilities.

1.4 Research Hypothesis and Objectives

We hypothesized that a floating, solar-powered multi-stage system integrating immobilized TiO₂ photocatalysis, strong-base anion exchange resin, GAC adsorption, and fine filtration would achieve significantly greater reductions in turbidity, TDS, and PFAS than a GAC-and-filtration-only control under natural winter sunlight. Specific objectives included evaluating turbidity, TDS, pH, and PFAS across three independent field trials; comparing full-system and GAC-only performance with effect size analysis; examining the expected photocatalytic contribution to microbial inactivation using literature-based UV dose estimation; and assessing cost and scalability for decentralized deployment.

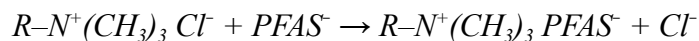
2. Background and Literature Review

2.1 TiO_2 Photocatalysis: Mechanism and Barriers

TiO_2 photocatalysis generates electron–hole pairs under UV irradiation that react with dissolved water and oxygen to produce hydroxyl radicals ($\bullet\text{OH}$, +2.80 V), superoxide radical anions, and hydrogen peroxide, collectively mineralizing organic pollutants to CO_2 and H_2O [2, 4]. ROS additionally inactivates pathogens through oxidative damage to cell membranes, proteins, and DNA, a mechanism extensively documented in the photocatalytic disinfection literature [4, 13]. Three barriers have limited field deployment of TiO_2 photocatalysis: nanoparticle release into treated water when suspended rather than immobilized; absorption primarily in the UV range (~5% of solar spectrum); and the inability to mineralize the C–F bond in PFAS under passive solar irradiance, necessitating a complementary selective separation stage [5, 10]. Reactor geometry is as critical as material properties: thin-film flow configurations, which spread water across coated surfaces in a thin layer rather than pooling, maximize both surface contact and light penetration under low-pressure solar conditions.

2.2 PFAS Chemistry, GAC Limitations, and Ion Exchange Removal

At environmental pH, PFOA and PFOS exist as anions through deprotonation of their carboxylate ($-\text{COO}^-$) and sulfonate ($-\text{SO}_3^-$) groups. GAC adsorption has been widely studied for PFAS removal: under optimal conditions with Empty Bed Contact Times of 5–25 minutes, coconut-shell GAC can achieve >95% removal of PFOS and PFOA in column studies [15]. However, GAC’s PFAS removal is highly kinetically limited; at contact times on the order of seconds, adsorption of PFAS onto GAC surfaces is minimal because the diffusion-limited transport of PFAS molecules into GAC micropores requires extended contact to approach equilibrium [15, 14]. This kinetic dependence has direct implications for HelioPure’s design, as discussed in Section 5.2. Strong-base anion exchange resins functionalized with quaternary ammonium groups ($-\text{N}^+(\text{CH}_3)_3$) capture PFAS anions through two simultaneous mechanisms: electrostatic attraction to fixed cationic sites displacing weaker counter-ions:



and hydrophobic partitioning of fluorinated tails into the polystyrene–divinylbenzene (PS-DVB) polymer matrix, a dual mechanism that preferentially removes longer-chain PFAS species [8].

Appleman et al. [9] validated this at full treatment plant scale, confirming effective PFAS removal across a range of hydraulic conditions. Critically, unlike GAC, ion exchange adsorption is not strongly kinetically limited for charged species under the electrostatic attraction mechanism: electrostatic capture occurs rapidly at resin surfaces, making it more suitable for short contact times than physisorption-based GAC removal [8].

2.3 Multi-Stage Synergy

The design philosophy of HelioPure rests on the empirically demonstrated principle that sequential treatment stages substantially outperform any single mechanism in isolation. TiO_2 photocatalysis contributes synergistically in two ways: by mineralizing dissolved organic macromolecules into CO_2 and water, as documented in the photocatalytic literature (directly reducing TDS), and by generating smaller, more polar oxidized fragments with higher GAC adsorption affinity, reducing organic load on downstream stages and extending GAC bed life. The anion exchange stage operates orthogonally through electrostatic and hydrophobic mechanisms entirely distinct from photocatalytic oxidation or GAC adsorption, providing a dimension of PFAS selectivity that neither of the other stages offers [8, 9].

3. Materials and Methods

3.1 Materials and System Design

HelioPure was designed under real-world constraints: no grid electricity, no chemical inputs, autonomous operation, surface water intake, field portability, and buildability without laboratory facilities from commercially available components. The photocatalytic reaction chamber was constructed from a clear acrylic tube (OLYCRAFT, 2.2" OD, 2.0" ID, 9.8" length) selected for UV transparency and mechanical durability. Research-grade anatase TiO_2 nanopowder (XFNANO, ~20–40 nm, 99% purity) was immobilized using J-B Weld ClearWeld epoxy (25 mL, 3,900 PSI tensile strength) onto three pre-cleaned glass microscope slides (3" \times 1"). Coconut shell-derived GAC (MAQIHAN, 410 g, pellet form, ~100 g loaded) provided the adsorption stage. The strong-base quaternary ammonium-functionalized PS-DVB anion exchange resin (~200 g loaded) provided PFAS-selective removal. The system was housed in an IRIS USA WeatherPro 47 Qt container (31.88" \times 19.88" \times 6.38"). Power was supplied by a Soshine 6W monocrystalline solar panel and ROMOSS Sense 8+ 30,000 mAh power bank. Internal components were connected via 0.5" food-grade tubing with

epoxy-sealed joints. Water quality was measured using a VIVOSUN Digital pH/TDS Meter Kit (± 0.01 pH, $\pm 2\%$ TDS readout) and a Droplet Turbidity Meter (20.0–200.0 NTU, resolution 0.1 NTU, ESPL). Total prototype materials cost was approximately \$165.

3.2 TiO₂ Immobilization

TiO₂ nanopowder and ClearWeld epoxy were combined in an approximate 1:1 volumetric ratio and applied to slide surfaces using a wooden applicator to a coating thickness of approximately 2–4 mm, then cured at room temperature for a minimum of one hour. The epoxy matrix approach was selected over sol-gel or dip-coating methods because it is reproducible without laboratory conditions and provides durable adhesion under continuous aqueous exposure [10]. No formal characterization of coating crystalline phase, surface area, or uniformity was performed, as these techniques require laboratory instrumentation unavailable in this study; these measurements represent important additions for future work to quantify catalytic activity per unit surface area. The 5-micron stainless steel mesh final filtration stage provided a secondary physical barrier against any TiO₂ particles reaching the treated water reservoir.

3.3 System Construction and Iterative Design

Construction spanned approximately seven months across six total design cycles. Version 1 development began in August 2025 and reached field-testable state by late November 2025 (Figure 6). Key V1 challenges included fabricating a waterproof pump mount under submerged conditions, precision cutting the acrylic tube for watertight integration, and resolving the filtration stage design: an initial 0.22 μm membrane filter failed due to complete flow blockage under the 5V pump's low pressure, resolved through four redesign iterations to a 5-micron stainless steel mesh. Version 2 began after regional science fair evaluation (in Feb 2026) and was completed in March 2026 (Figure 7), adding a horizontally oriented PVC anion exchange cartridge compressed with metal fasteners to minimize void fraction, retained by stainless steel micron-mesh screens, and isolated by a fine polymer separator. The final V2 flow path: surface water intake \rightarrow 5V pump \rightarrow TiO₂ chamber (15° angle, ~ 15 sec contact) \rightarrow anion exchange cartridge (~ 20 sec contact) \rightarrow GAC column \rightarrow 5-micron mesh \rightarrow 3.3L storage reservoir. Contact times in each stage were measured using a stopwatch by timing water transit through each component at the system's operating flow rate, calculated from the observed time to fill the 3.3L

reservoir. The system operated at an approximate flow rate of 130 mL/min, yielding an estimated GAC EBCT of under 60 seconds.

3.4 Field Testing Protocol

Testing was conducted at a small residential freshwater lake on Lochaven Road, Waxhaw, North Carolina, a private natural pond set within a wooded residential community fed by local surface runoff. Turbidity and TDS trials were conducted in mid-December 2025 between 12:00 and 14:00 under clear winter sunlight. PFAS trials were conducted in late January 2026 under comparable clear winter conditions at the same location; the separate test dates are acknowledged as a methodological limitation (Section 5.5). For each trial, baseline measurements were taken at the lake surface; the HelioPure unit was deployed and operated for 20–30 minutes until the treated-water reservoir was filled; treated water was collected and analyzed. The identical water source was used simultaneously for both the full system and the GAC-only control to eliminate source variability. Three independent trials were conducted per configuration.

3.5 PFAS Quantification and Statistical Analysis

PFAS concentrations were quantified using the Cyclopure PFAS Water Test Kit Pro (DEXSORB cyclodextrin solid-phase extraction; HPLC-MS/MS with isotope dilution; validated against EPA Methods 533, 537, and 1633; LOQ 1.0 ppt for 54 analytes). Influent and effluent samples were collected in triplicate across three independent trials. Mean removal efficiencies and standard deviations were calculated from three trials per parameter. Full-system versus GAC-only differences were evaluated using two-sample t-tests (significance at $p < 0.05$). PFAS significance was assessed by two-sample t-test comparing influent and effluent concentrations. Given $n=3$ per group, effect sizes (Cohen's d) were calculated from pooled standard deviations to supplement p-values: turbidity $d = 5.5$, TDS $d = 4.3$, PFAS $d = 14.9$, all indicating very large to extremely large effects that remain meaningful despite small sample size. Error bars represent \pm one standard deviation.

4. Results

4.1 Turbidity Reduction

Raw surface water exhibited turbidity values of 93.4, 102.8, and 82.6 NTU across the three trials. The full HelioPure system reduced turbidity to 20.7, 21.1, and 20.4 NTU, a mean reduction of $78.4\% \pm 2.1\%$ (Figure 1; Table 1). The GAC-only control reduced turbidity to 23.8, 25.6, and 24.4 NTU, a mean reduction of approximately 73.5% ($p < 0.05$, two-sample t-test; $d = 5.5$). The consistent convergence of full-system outputs toward the 20.0 NTU instrument detection limit across all three independent trials suggests that actual post-treatment turbidity may have been below the measurable threshold, meaning the reported 78.4% may underestimate true turbidity reduction; this cannot be confirmed without a lower-LOD instrument. Visual inspection supported this trend: full-system output exhibited near-complete clarification to a bottled-water-like quality, while GAC-only output retained faint residual turbidity and slight color under direct light (Figure 2).

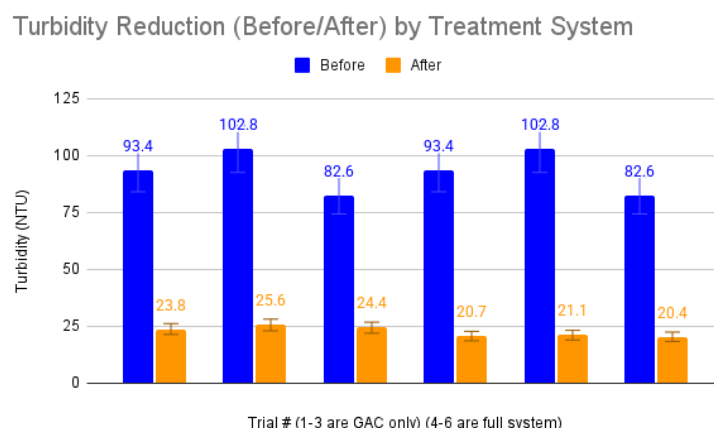


Figure 1. Turbidity reduction across three independent trials. Dark blue: before treatment. Orange: after full system treatment. Light blue: after GAC-only treatment. Mean full-system reduction: $78.4\% \pm 2.1\%$; GAC-only: 73.5%. Error bars: \pm one SD ($n = 3$). Full system significantly outperformed GAC-only ($p < 0.05$; $d = 5.5$). Instrument lower detection limit: 20.0 NTU.

4.2 TDS Reduction

Initial TDS ranged from 562 to 617 ppm. The full system reduced TDS to 301, 304, and 298 ppm, a mean reduction of $50.1\% \pm 1.9\%$. The GAC-only control achieved 425, 483, and 397 ppm, a mean reduction of approximately 28–35% (Figure 3; Table 1; $p < 0.05$; $d = 4.3$). The 15–22% additional TDS reduction observed in the full system compared to the GAC-only control is attributable to the combined contribution of the TiO_2 photocatalytic and anion exchange stages, both of which were present in the full

system but absent in the control. TiO_2 photocatalysis plausibly contributes through oxidative mineralization of dissolved organics to CO_2 and water, and through conversion of large organic molecules into smaller, more polar fragments with higher GAC adsorption affinity. The anion exchange resin contributes through capture of dissolved anionic species. Because these two stages were not independently isolated in separate trials, the contribution of each to TDS reduction cannot be disaggregated from the existing dataset and is acknowledged as a limitation; a third experimental configuration (TiO_2 +GAC without ion exchange) would be needed to isolate the photocatalytic contribution specifically.

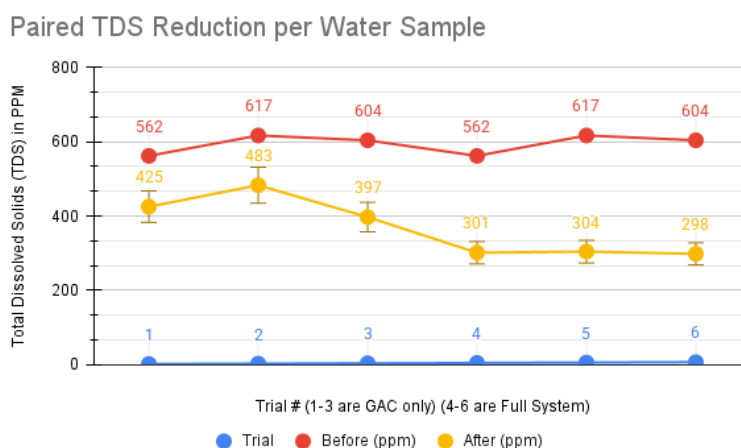


Figure 3. TDS reduction across three independent trials. Mean full-system reduction: $50.1\% \pm 1.9\%$ (298–304 ppm from 562–617 ppm initial). GAC-only: 28–35% (397–483 ppm). The combined photocatalytic and ion exchange stages contributed an additional 15–22% reduction beyond GAC-filtration alone ($p < 0.05$; $d = 4.3$). Error bars: \pm one SD ($n = 3$).

4.3 pH Stability

pH remained within 7.61–7.84 across all trials and configurations. The full system produced a mean shift of -0.18 pH units; the GAC-only control produced -0.11 units. Both values fall well within the WHO potable water guideline range of 6.5–8.5, confirming that ROS generated during TiO_2 photocatalysis were transient and did not accumulate as acidic byproducts.

4.4 PFAS Removal

Influent PFAS concentrations were 54.68, 63.23, and 59.44 ppt, yielding a mean of 59.12 ± 3.54 ppt. Post-treatment effluent concentrations were 7.65, 11.37, and 8.09 ppt, yielding a mean of 9.04 ± 1.67 ppt.

ppt. Mean removal efficiency was $84.8\% \pm 2.0\%$ ($p < 0.001$; $d = 14.9$; Figure 4; Table 1). This result was obtained under passive solar operation with approximately 20 seconds of resin contact time, near-atmospheric pressure, a tannin-reduction resin not specifically optimized for PFAS, in real untreated surface water under December–January solar conditions, without laboratory facilities. The anion exchange stage was primarily responsible for PFAS removal based on the mechanistic distinction between ion exchange and GAC: unlike physisorption of PFAS onto GAC micropores - which is kinetically limited and requires Empty Bed Contact Times of 5–25 minutes for meaningful removal [15] - electrostatic capture by quaternary ammonium groups occurs rapidly at resin surfaces. At HelioPure's GAC contact time of seconds rather than minutes, literature predicts minimal PFAS removal from the GAC stage alone [15, 8]. The absence of a GAC-only PFAS control trial is acknowledged as a methodological limitation and is the highest-priority experimental addition for future study; however, the kinetic argument from the established literature provides a reasonable mechanistic basis for attributing the observed removal primarily to the ion exchange stage. Trial 2's higher effluent (11.37 ppt at 63.23 ppt influent) relative to Trials 1 and 3 is consistent with concentration-dependent ion exchange equilibrium behavior, not resin exhaustion. Mean effluent of 9.04 ppt remains above the EPA's 4.0 ppt MCL; 84.8% reduction from ~59 ppt represents a meaningful public health intervention where no alternative treatment is available.

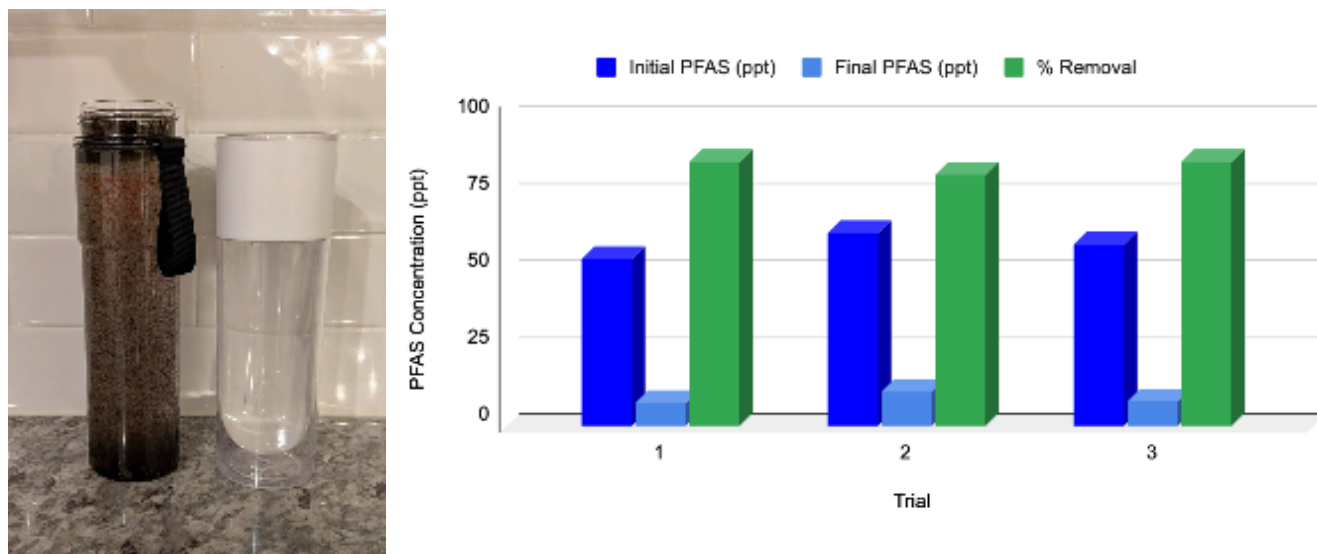


Figure 2. (Left) Visual comparison of untreated surface water (left) and HelioPure full-system treated water (right) from the same trial. Treated water exhibited near-complete clarification consistent with the quantitative turbidity reduction of 78.4% reported in Figure 1.

Figure 4. (Right) PFAS reduction across three independent trials. Dark blue: influent (ppt). Light blue: effluent (ppt). Green: percent removal. Mean influent: 59.12 ± 3.54 ppt; mean effluent: 9.04 ± 1.67 ppt; mean removal: $84.8\% \pm 2.0\%$ ($p < 0.001$; $d = 14.9$; $n = 3$). PFAS quantified by Cyclopure laboratory: HPLC-MS/MS, isotope dilution, EPA Methods 533/537/1633 validated. LOQ: 1.0 ppt for 54 analytes. EPA MCL: 4.0 ppt.

4.5 Summary Data

	Turbidity Before (NTU)	Turbidity After: Full (NTU)	TDS Before (ppm)	TDS After: Full (ppm)	pH Before	pH After: Full	PFAS Before (ppt)	PFAS After (ppt)
Trial 1	93.4	20.7	562	301	7.78	7.63	54.68	7.65
Trial 2	102.8	21.1	617	304	7.83	7.61	63.23	11.37
Trial 3	82.6	20.4	604	298	7.84	7.65	59.44	8.09
	Turbidity Before (NTU)	Turbidity After: GAC (NTU)	TDS Before (ppm)	TDS After: GAC (ppm)	pH Before	pH After: GAC	N/A Control not tested for PFAS	N/A Control not tested for PFAS
Trial 1	93.4	23.8	562	425	7.78	7.69		
Trial 2	102.8	25.6	617	483	7.83	7.72		
Trial 3	82.6	24.4	604	397	7.84	7.71		

Table 1. Complete water quality data across three independent trials. Upper panel: full HelioPure system (TiO_2 photocatalysis + anion exchange + GAC + filtration). Lower panel: GAC-and-filtration-only control. PFAS measurement was not performed on the GAC-only configuration; the rationale for attributing PFAS removal primarily to the anion exchange stage based on kinetic arguments from the literature is discussed in Section 5.2.

5. Discussion

5.1 System Performance and Photocatalysis–Adsorption Synergy

The results support the central hypothesis. Across all three independent field trials, the integrated system achieved statistically significant improvements over the GAC-only control in turbidity and TDS removal, with pH stability confirming chemical safety. The large effect sizes (turbidity $d = 5.5$, TDS $d =$

4.3) indicate that despite $n=3$, the observed differences are of sufficient magnitude to be meaningful beyond chance. TDS reduction in the full system exceeded the GAC-only control by 15–22%; this additional reduction is attributable to the combined contribution of the TiO_2 photocatalytic and ion exchange stages, not to photocatalysis alone, as both stages were present in the full system but absent in the control. A dedicated three-configuration experiment (full system, TiO_2 +GAC only, GAC only) would be required to disaggregate the individual contributions of photocatalysis and ion exchange to TDS reduction, and this represents a clear priority for future experimental design.

5.2 PFAS Removal: Attribution and Significance

The 84.8% mean PFAS removal ($d = 14.9$) achieved under passive solar conditions is this study's most significant contribution. The absence of a GAC-only PFAS control trial is the most important methodological limitation in the dataset; without it, PFAS removal technically cannot be experimentally attributed exclusively to the anion exchange stage. This limitation is directly and explicitly acknowledged. However, the literature provides strong mechanistic grounds for the attribution. PFAS removal by GAC is primarily governed by kinetically slow physisorption into micropores, requiring EBCTs of 5–25 minutes for meaningful removal in column studies [15, 14]. At HelioPure's operating flow rate, the GAC contact time was on the order of seconds: two to three orders of magnitude shorter than the minimum effective EBCT. Deng et al. [8] additionally demonstrated that anion exchange resin consistently outperforms GAC for PFAS removal at equivalent contact times due to the kinetic advantage of electrostatic vs. diffusion-limited mechanisms. Under HelioPure's operating conditions, the expected GAC contribution to PFAS removal is minimal based on this literature, supporting the conclusion that the anion exchange resin was the dominant removal mechanism. Running the GAC-only PFAS control trial remains the highest-priority experimental addition for the next study phase, both to confirm this attribution and to quantify the net ion exchange contribution precisely.

To contextualize the result: consumer-grade GAC filters provide negligible PFAS removal for long-chain species at typical point-of-use contact times. Reverse osmosis achieves 90–96% removal but requires 50–150 psi, membrane maintenance, and reject stream management. HelioPure achieved 84.8% at near-atmospheric pressure, passive solar power, no reject stream, with a non-PFAS-optimized resin, in real untreated surface water under winter solar conditions, without laboratory facilities. The extremely

large effect size ($d = 14.9$) across three trials indicates that the PFAS result is robust, though larger n would strengthen statistical confidence.

5.3 Photocatalytic Microbial Inactivation: Evidence-Based Projection

Microbial inactivation was not directly measured in this study, as culture-based pathogen assays require laboratory equipment unavailable to independent researchers. This is an acknowledged limitation. Rather than projecting 1–2 log reduction without qualification (as previous versions of this paper stated), a UV dose–based analysis is presented to bound the plausible photocatalytic disinfection effect under actual operating conditions.

At 35°N latitude during the 12:00–14:00 December-January testing window, clear-sky UV-A irradiance is approximately 10–15 W/m² at ground level [13]. For a 15-second single pass through the photocatalytic chamber, the approximate UV-A dose delivered to TiO₂-coated surfaces is therefore 10–15 W/m² × 15 sec = 150–225 J/m². By comparison, Rizzo et al. [11] - demonstrating 93.17% *E. coli* inactivation in 10 minutes under simulated solar TiO₂ conditions - used an effective UV-A irradiance substantially exceeding typical winter conditions at 35°N, with a delivered dose estimated at 18,000+ J/m². HelioPure's single-pass UV dose (~150–225 J/m²) is therefore approximately 80–120× lower than that study's effective dose. Projecting the 1-2 log inactivation from Rizzo et al. onto HelioPure's single-pass conditions is not supported by this UV dose comparison.

A more defensible interpretation is that HelioPure's TiO₂ stage initiates ROS-mediated membrane oxidation and sub-lethal cell damage during the 15-second contact period, creating a bacteriostatic effect and reducing viable pathogen populations, but complete 1-2 log inactivation in a single pass under winter solar conditions is unlikely. Complete inactivation would require either a recirculation loop (which the V3 design could incorporate by adding a bypass valve) or an extended-contact TiO₂ section with more coated slides. Direct quantitative microbial assay (culture-based *E. coli* enumeration or qPCR pathogen detection) is a necessary experimental priority for the next phase. The photocatalytic disinfection literature strongly supports this as a valuable and achievable system capability; demonstrating it with actual data is what remains to be done.

5.4 Cost Analysis

HelioPure's prototype cost was approximately \$165 complete; approximately \$100–110 for actually consumed material quantities. At industrial production scale, commercial-grade anatase TiO₂ costs ~\$3–5/kg (versus ~\$200/kg for research-grade nanopowder); industrial GAC costs ~\$1–2/kg; and solar panels cost ~\$0.20–0.30/W at scale, producing an estimated unit cost of \$30–40. Cost per liter of treated water, estimated at \$0.001–0.005, is derived from assumptions of 40–60 L/day production over a 2-year lifespan with quarterly consumable replacement at ~\$10–15. These assumptions carry significant uncertainty: resin exhaustion timelines were not characterized, and TiO₂ coating longevity has not been evaluated. The cost estimate is therefore best understood as a rough illustrative projection under plausible operating assumptions, not a validated engineering estimate. Formal cost modeling with measured flow rate and media longevity data is required for a rigorous lifecycle cost analysis.

5.5 Limitations

The following limitations are explicitly acknowledged. (1) No GAC-only PFAS control was run; PFAS removal attribution to ion exchange relies on kinetic arguments from the literature rather than direct experimental evidence. (2) $n=3$ per configuration provides low statistical power; while effect sizes are large ($d = 4.3$ – 14.9), larger n would improve confidence. (3) PFAS trials were conducted on a separate date (late January 2026) from turbidity/TDS trials (mid-December 2025); water chemistry may have differed seasonally. (4) A third experimental configuration isolating the photocatalytic contribution to TDS reduction was not tested. (5) Turbidity measurements were constrained by the 20.0 NTU instrument floor; reported 78.4% reduction may underestimate true performance. (6) Microbial inactivation was not measured, and single-pass UV dose analysis indicates the projection of 1–2 log reduction overstated plausible performance under winter solar conditions at 15-second contact time. (7) No TiO₂ coating characterization (XRD, BET surface area, adhesion testing) was performed. (8) Testing was conducted at a single site under December–January solar irradiance; generalizability to other water chemistries, seasons, and latitudes has not been demonstrated. (9) Cost estimates rely on unverified operational assumptions. (10) Resin exhaustion rates and TiO₂ coating durability under extended deployment have not been evaluated.

5.6 Future Directions

Experimental priorities in order of importance: (1) GAC-only PFAS control trial to directly quantify the anion exchange stage's contribution; (2) quantitative microbial assay with culture-based *E. coli* enumeration; (3) third treatment configuration (TiO_2 +GAC, no ion exchange) to isolate photocatalytic TDS contribution; (4) resin longevity characterization; (5) TiO_2 coating characterization; (6) multi-site and multi-season testing. A scaled 10-liter V3 design is currently under active development, replacing the separate internal storage container with a rigid internal flow barrier, incorporating foam exterior inserts for enhanced buoyancy, and extending resin bed and GAC mass for improved contact time and per-pass removal. The most personally significant planned deployment is a field test in Tirunelveli, Tamil Nadu, India in summer 2026, testing on the surface water bodies used by local communities that motivated this research, with local leaders engaged as evaluation partners. This deployment will generate data under conditions genuinely different from a North Carolina residential lake: different water chemistry, higher turbidity, higher temperatures, and a context where safe water access has immediate public health significance. Potential future collaboration with scientists such as Dr. Courtney Di Vittorio at Wake Forest University, whose satellite-based water quality monitoring of NC water bodies could inform HelioPure deployment site prioritization at landscape scale, represents an additional direction for extending this work beyond individual system testing.

6. Conclusion

HelioPure demonstrates that solar-driven photocatalysis and ion exchange chemistry can be integrated into a field-deployable, infrastructure-independent purification platform using commercially available materials, without laboratory facilities, at a prototype cost of approximately \$165. Across three independent field trials, the system achieved 78.4% turbidity reduction, 50.1% TDS reduction, and 84.8% PFAS removal in real untreated surface water under natural winter solar conditions, with large to very large effect sizes confirming the practical significance of these differences relative to a GAC-only control. The system's design honestly confronts the methodological limitations of independent research: the missing GAC-only PFAS control, the $n=3$ dataset, the absence of microbial data, and the uncharacterized coating properties are all acknowledged as gaps requiring future experimental attention. These limitations do not undermine the core findings but define the specific work needed to elevate this study from compelling preliminary evidence to comprehensive validation.

The innovation in HelioPure is systems integration: taking photocatalysis, confined largely to controlled reactors for decades, and combining it with ion exchange separation in a form factor that floats on the water it treats, powers itself from sunlight, and can be built from a hardware store. The PFAS result (84.8% removal at sub-minute ion exchange contact time, near-atmospheric pressure, without laboratory facilities, in real surface water) establishes that this level of chemical treatment is achievable under decentralized conditions. Whether that finding holds across multiple sites, seasons, and water chemistries; how long the resin and coating last; and whether microbial inactivation accompanies chemical removal; these are the questions the next generation of HelioPure experiments will answer, beginning with a planned field deployment in the Tirunelveli community that I felt first made this research feel necessary.

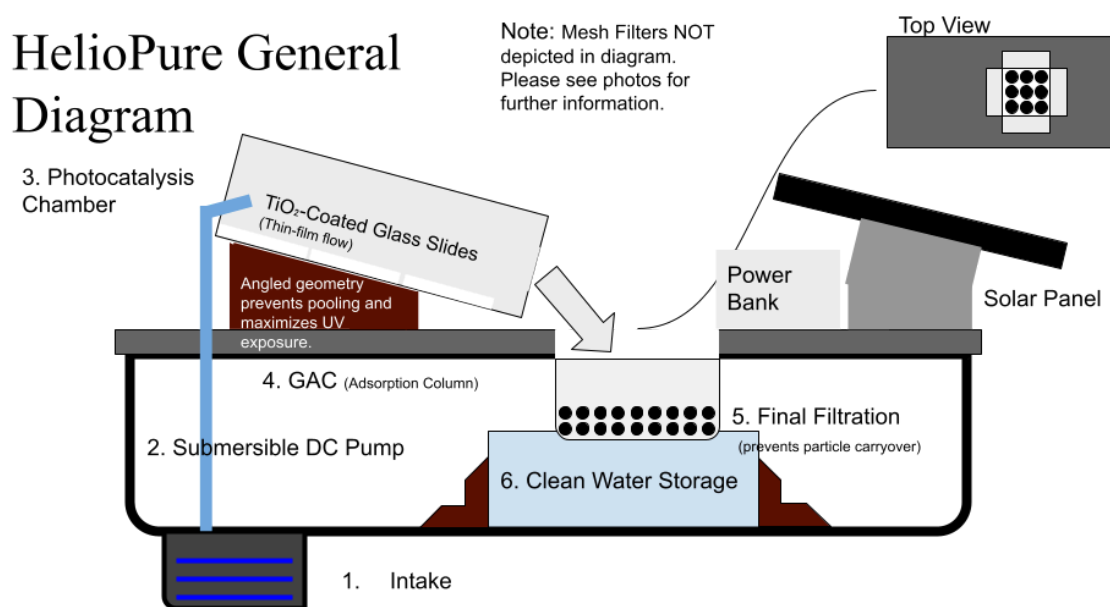


Figure 5. HelioPure V1 system schematic: (1) surface water intake via submersible 5V DC pump; (2) TiO₂-coated glass slides in 15°-angled acrylic photocatalytic chamber (~15 sec contact); (3) GAC adsorption column (100 g coconut shell); (4) 5-micron stainless steel mesh final filtration barrier; (5) 3.3L treated-water storage reservoir. Powered by 6W monocrystalline solar panel and 30,000 mAh power bank. Mesh filtration components omitted for clarity.

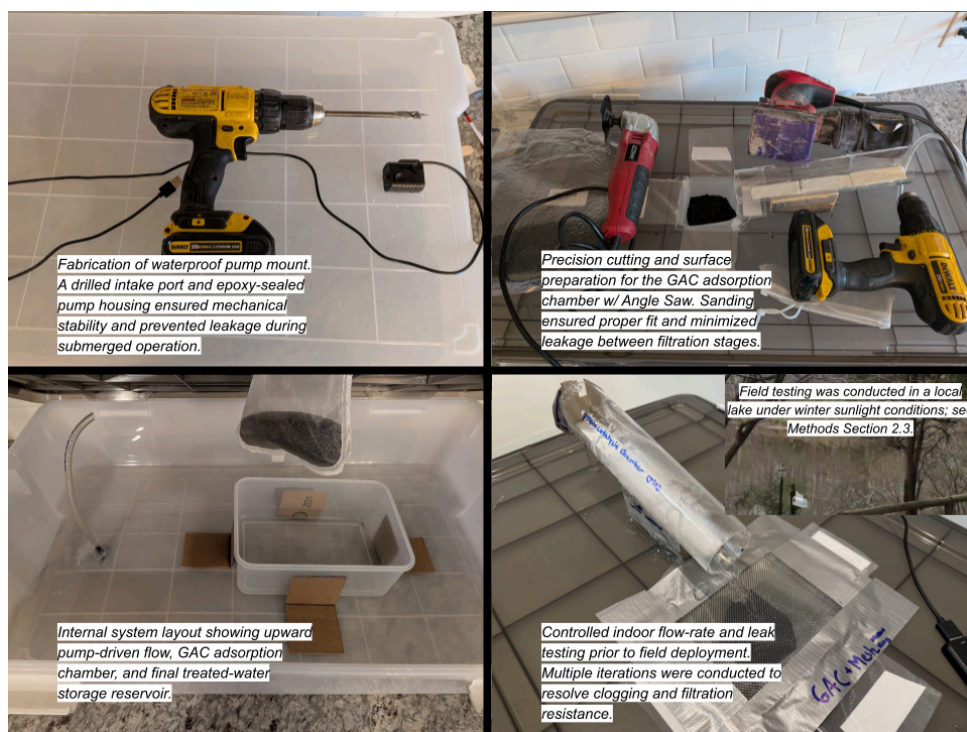


Figure 6. HelioPure V1 construction.

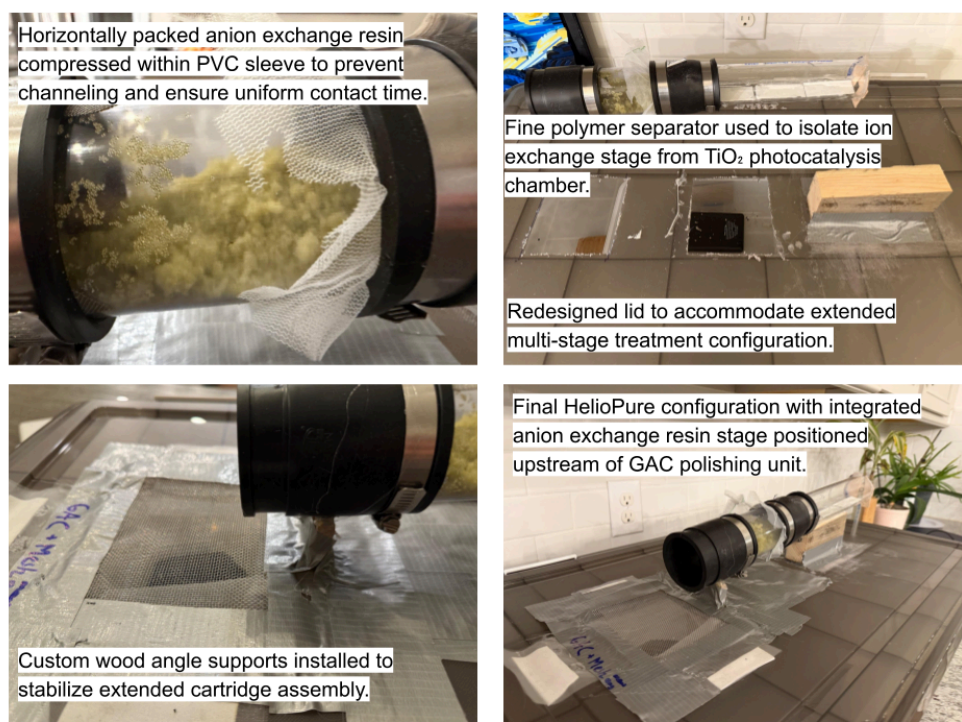


Figure 7. HelioPure V2 construction.

References

1. World Health Organization and UNICEF. “Progress on household drinking water, sanitation and hygiene 2000–2020.” *WHO/UNICEF Joint Monitoring Programme*, 2021. <https://washdata.org> Accessed 1 Apr. 2026.
2. Fujishima, A., et al. “TiO₂ photocatalysis: fundamentals and applications.” *Journal of Photochemistry and Photobiology C: Photochemistry Reviews*, vol. 1, no. 1, 2000, pp. 1–21. [https://doi.org/10.1016/S1389-5567\(00\)00002-2](https://doi.org/10.1016/S1389-5567(00)00002-2)
3. U.S. Environmental Protection Agency. “PFAS explained.” *EPA*, 2024. <https://www.epa.gov/pfas> Accessed 1 Apr. 2026.
4. Chong, M. N., et al. “Recent developments in photocatalytic water treatment technology: a review.” *Water Research*, vol. 44, no. 10, 2010, pp. 2997–3027. <https://doi.org/10.1016/j.watres.2010.02.039>
5. Chen, X., and S. S. Mao. “Titanium dioxide nanomaterials: synthesis, properties, modifications, and applications.” *Chemical Reviews*, vol. 107, no. 7, 2007, pp. 2891–2959. <https://doi.org/10.1021/cr0500535>
6. U.S. Environmental Protection Agency. “National primary drinking water regulation for PFAS.” *EPA*, 2023. <https://www.epa.gov/sdwa/and-polyfluoroalkyl-substances-pfas> Accessed 1 Apr. 2026.
7. Shannon, M. A., et al. “Science and technology for water purification in the coming decades.” *Nature*, vol. 452, 2008, pp. 301–310. <https://doi.org/10.1038/nature06599>
8. Deng, S., et al. “Removal of perfluorinated compounds from aqueous solution by ion exchange resins: adsorption mechanism and capacity.” *Environmental Science & Technology*, vol. 44, no. 9, 2010, pp. 3571–3576. <https://doi.org/10.1021/es100567v>
9. Appleman, T. D., et al. “Treatment of poly- and perfluoroalkyl substances in U.S. full-scale water treatment systems.” *Water Research*, vol. 51, 2014, pp. 246–255. <https://doi.org/10.1016/j.watres.2013.10.067>
10. Zhao, J., et al. “Immobilized TiO₂ photocatalysts for water treatment: a review.” *Catalysis Today*, vol. 224, 2014, pp. 76–85. <https://doi.org/10.1016/j.cattod.2013.10.014>
11. Rizzo, L., et al. “Disinfection of urban wastewater by solar driven and UV lamp–TiO₂ photocatalysis: effect on a multi drug resistant *Escherichia coli* strain.” *Water Research*, vol. 53, 2014, pp. 145–152. <https://doi.org/10.1016/j.watres.2014.01.020>

12. Salih, F. M. “Enhancement of solar inactivation of *Escherichia coli* by titanium dioxide photocatalytic oxidation.” *Journal of Applied Microbiology*, vol. 92, 2002, pp. 920–926.
<https://doi.org/10.1046/j.1365-2672.2002.01613.x>
13. Malato, S., et al. “Decontamination and disinfection of water by solar photocatalysis: recent overview and trends.” *Catalysis Today*, vol. 147, 2009, pp. 1–59.
<https://doi.org/10.1016/j.cattod.2009.06.018>
14. Crittenden, J. C., et al. *Water Treatment: Principles and Design*, 3rd ed., Wiley, 2012.
15. McNamara, J. D., et al. “Comparison of activated carbons for removal of perfluorinated compounds from drinking water.” *Journal AWWA*, vol. 110, no. 1, 2018, pp. E3–E14.
<https://doi.org/10.5942/jawwa.2018.110.0003>
16. Krishna, A. P. “PuriFAS: A Fast Action System for PFAS Removal.” *NSRI Student Research Journal X MIT Critical Data*, 2026.
17. Du, Z., et al. “Adsorption behavior and mechanism of perfluorinated compounds on various adsorbents.” *Chemical Engineering Journal*, vol. 253, 2014, pp. 144–152.
<https://doi.org/10.1016/j.cej.2014.05.035>
18. Helfferich, F. *Ion Exchange*. Dover Publications, 1995.
19. Clara, M., et al. “Emissions of perfluorinated alkylated substances (PFAS) from point sources.” *Water Research*, vol. 43, no. 17, 2009, pp. 4051–4062.
<https://doi.org/10.1016/j.watres.2009.06.014>
20. World Health Organization. “Drinking-water.” *WHO Fact Sheets*, 2022.
<https://www.who.int/news-room/fact-sheets/detail/drinking-water> Accessed 1 Apr. 2026.